PHYSICAL REVIEW B VOLUME 27, NUMBER 9 1 MAY 1983

Amplitude-fluctuation effects on magnetic-resonance line shape and soliton density in incommensurate systems

R. Blinc and P. Prelovšek
J. Stefan Institute, Department of Physics, E. Kardelj University of Ljubljana, 61000 Ljubljana, Yugoslavia

R. Kind
Laboratory of Solid State Physics, Swiss Federal Institute of Technology, Hönggerberg, CH-8093 Zürich, Switzerland

(Received 1 October 1982)

The magnetic-resonance line shape in one-dimensionally modulated structurally incommensurate systems has been evaluated for the case of a multisoliton lattice taking into account both phase and amplitude variations in space. Amplitude variations significantly affect the NMR line shape outside the "plane-wave" regime. A comparison is made between the temperature dependence of the average incommensurate wave vector and the soliton density in the constant-amplitude approximation and in the case when amplitude variations are taken into account.

I. INTRODUCTION

Structurally incommensurate (I) systems have been, by now, extensively investigated by magnetic-resonance techniques.[1] Instead of a small number of magnetic-resonance lines—arising from physically nonequivalent sites in the unit cell of translationally periodic crystals—one finds in I systems a quasicontinuous frequency distribution which reflects the spatial variation of the order parameter, i.e., of the frozen-out incommensurate soft mode. The condensation of the soft mode at the paraelectric (P)—incommensurate (I) transition T_I results in a superlattice, the periodicity of which is an irrational fraction of the periodicity of the underlying lattice. The translational invariance is lost in the direction of the I modulation and the whole crystal is a unit cell.[2]

Magnetic-resonance studies have shown that in most I systems in the high-temperature part of the I phase the frozen-out incommensurate modulation wave is pinned and can be described by a "plane wave." In the low-temperature part of the I phase the magnetic-resonance frequency distribution cannot be described anymore by this model. The spectra show the existence of nearly commensurate regions which are separated by static solitonlike "discommensurations" where the phase of the modulation wave changes rapidly. The density of the phase solitons goes to zero at the incommensurate (I)—commensurate (C) transition temperature T_c.

No experimental evidence has been found so far for the spatial variation of the amplitude of the order parameter though it is clear that the energy would decrease if the amplitude would be diminished at the position of the discommensuration.[2-4] It is the purpose of this paper to evaluate the effects of the spatial variations of the amplitude of the order parameter on the NMR line shape and the temperature dependence of the soliton density. By comparing experimental data with theoretical predictions one should be able to throw some light on amplitude variations occurring in addition to phase solitons.[2-4]

II. AMPLITUDE VARIATIONS IN SPACE

Let us treat the case of a one-dimensional incommensurate modulation. We shall assume that the incommensurate soft mode belongs to a two-dimensional irreducible representation and that a Lifshitz invariant is allowed by symmetry.[5] The free-energy density $g(x)$ can be written in the continuum limit in polar coordinates $\tilde{p}=A(x)\cos\phi(x)$, $\tilde{q}=A(x)\sin\phi(x)$ as

$$g(x)=\frac{\alpha}{2}A^2+\frac{\beta}{4}A^4+\gamma A^n\cos^2\left[\frac{n\phi}{2}\right] -\Lambda A^2\phi'+\frac{\kappa}{2}(A^2\phi'^2+A'^2)\,, \tag{1}$$

where $\phi'=\partial\phi/\partial x$, $A'=\partial A/\partial x$, $\alpha=\alpha_0(T-T_0)$, n is even, i.e., $n=4,6,8,\ldots$, and all other coefficients are assumed to be constants. The first two terms represent the standard Landau expansion in a homogeneous crystal. The γ term represents the anisotro-

py energy responsible for the lock-in transition at lower temperatures and has n minima for $0<\phi<2\pi$.

To simplify the analysis we have chosen the form containing $\cos^2(n\phi/2)$ and not the usual form with $\cos(n\phi)$. The difference, i.e., $\frac{1}{2}\gamma A^n$, represents a term of higher order. The Λ term represents the Lifshitz invariant inducing the transition to the I phase and the κ term represents the elastic energy stabilizing the homogeneous phase.

The minimization of the free energy—$F=(1/L)\int_0^L g(x)dx$, $\delta F=0$—leads to the Euler-Lagrange equations

$$\frac{\partial g}{\partial A}-\frac{d}{dx}\frac{\partial g}{\partial A'}=0\,, \tag{2a}$$

$$\frac{\partial g}{\partial \phi}-\frac{d}{dx}\frac{\partial g}{\partial \phi'}=0\,, \tag{2b}$$

yielding

$$\kappa A''=\alpha A+\beta A^3+n\gamma A^{n-1}\cos^2\left[\frac{n\phi}{2}\right]-2\Lambda A\phi'+\kappa A\phi'^2\,, \tag{3a}$$

$$(\kappa A^2\phi'-\Lambda A^2)=-\frac{n\gamma}{2}A^n\sin(n\phi)\,. \tag{3b}$$

The above coupled nonlinear differential equations for the amplitude A and the phase ϕ cannot be solved analytically. The phase equation (3b) can be solved exactly[2–4] if the amplitude is constant in space, $A=A_0$. In the following we assume that the amplitude variations around A_0 are small, i.e,

$$A=A_0+\Delta A(x),\ \Delta A(x)\ll A_0 \tag{4a}$$

and linearize Eq. (3a) with respect to ΔA. We obtain

$$\kappa\Delta A''=\left[\alpha+3\beta A_0^2+n(n-1)\gamma A_0^{n-2}\cos^2\left[\frac{n\phi}{2}\right]-2\Lambda\phi'+\kappa\phi'^2\right]\Delta A$$
$$=\alpha A_0+\beta A_0^3+n\gamma A_0^{n-1}\cos^2\left[\frac{n\phi}{2}\right]-2\Lambda A_0\phi'+\kappa A_0\phi'^2\,. \tag{4b}$$

Close to the *P-I* transition the *"plane-wave" approximation* is a good starting point and we find for $A=A_0=$const the first integral of the phase equation (3b) as

$$\phi'=q-\frac{\gamma}{2\Lambda}A_0^{n-2}\cos(nqx)\,, \tag{5a}$$

where we used on the right-hand side (rhs) of Eq. (3b) the approximation $\phi\approx qx$ with

$$q=q_0=\Lambda/\kappa\,. \tag{5b}$$

The amplitude A_0 is obtained from Eq. (4b) by the requirement that the inhomogeneous term [i.e., the right-hand side of Eq. (4b)] should vanish on the average. When we insert expression (5a), we obtain the well-known result

$$A_0=\left[\frac{\alpha_0}{\beta}(T_I-T)\right]^{1/2}, \tag{6a}$$

where the *P-I* transition temperature T_I is defined as

$$T_I=T_0+\Lambda^2/(\kappa\alpha_0)\,. \tag{6b}$$

Though the anisotropy term is small, it is essential for the appearance of amplitude variations. Therefore, we neglect on the left-hand side (lhs) of Eq. (4b) terms containing γ, but retain them on the rhs. Thus we get

$$\kappa\Delta A''-\xi\Delta A=-\frac{n\gamma}{2}A_0^{n-1}\cos(n\phi)\,, \tag{7a}$$

where

$$\xi\approx 2\beta A_0^2\,. \tag{7b}$$

The space-varying part of the amplitude is now obtained by inserting the plane-wave solution into (7a) as

$$\Delta A(x)=A_1\cos(nqx)\,, \tag{8a}$$

where

$$A_1\approx\frac{n\gamma A_0^{n-1}}{2(\xi+\kappa n^2q^2)}\,. \tag{8b}$$

Expressions (5), (8a), and (8b) describe the space variation of the amplitude and the phase in the plane-wave limit. The amplitude variations depend mainly on the anisotropy contribution and increase with increasing T_I-T.

In the low-temperature part of the I phase the plane-wave approximation breaks down and we have a *multisoliton lattice.* In the limit where the intersoliton spacing is large as compared to the soliton width, we find[2] from Eq. (3b) in the $A=A_0$ approximation the single-soliton solution as

$$\phi(x)=\frac{4}{n}\arctan\left[\exp\left[\frac{n(\gamma A_0^{n-2})^{1/2}}{\sqrt{2\kappa}}x\right]\right]-\frac{\pi}{n}\,,$$
$$x\in[-\infty,+\infty]\,. \quad (9)$$

The I-C transition temperature T_c is obtained from the condition for the marginal stability of the single soliton at $T=T_c$:

$$A_0^{(n-2)/2}=\frac{\pi}{2}\frac{\Lambda}{\sqrt{2\gamma\kappa}}\,. \quad (10)$$

The amplitude variation over the phase soliton—separating regions with $\phi=-\pi/n$ from regions with $\phi=\pi/n$—is now calculated for the case of a broad I phase where $T_I-T_c\gg T_I-T_0$ from a simplified form of Eq. (4b):

$$\kappa\Delta A''-\xi\Delta A=A_0G[\phi(x)]\,, \quad (11)$$

where ξ is again given by Eq. (7b) and

$$G(\phi(x))=\frac{\pi\Lambda^2}{\kappa}\left[\frac{(n+2)\pi}{8}\cos^2\left[\frac{n\phi}{2}\right]+\cos\left[\frac{n\phi}{2}\right]\right]. \quad (12)$$

When we insert in $G(\phi(x))$ the known solution for $\phi(x)$, Eq. (10) can be solved by the Green's-function method

$$\Delta A(x)=-A_0\int_{-\infty}^{+\infty}dx_0G(\phi(x_0))\frac{1}{\sqrt{\xi\kappa}}\times\exp\left[-\left[\frac{\xi}{\kappa}\right]^{1/2}|x-x_0|\right]. \quad (13)$$

The above relation between the space variation of the amplitude of the order parameter $\Delta A(x)$ and the phase $\phi(x)$ is a nonlocal one. Expression (13) reduces to a local relation in the case of a broad I phase where $\sqrt{\kappa/\xi}$ is much smaller than the soliton width. In this case the kernel of the integral (13) can be approximated by a δ function and we find

$$\frac{\Delta A(x)}{A_0}=-\frac{1}{\xi}G(\phi(x))\propto\gamma^{2/(n-2)}\,. \quad (14)$$

At least at the center of the soliton $G(\phi)$ is positive and $\Delta A(x)$ is negative. The amplitude of the order parameter will thus decrease in the region where the phase varies rapidly. This agrees with the numerical analysis of the coupled amplitude-phase problem.[4,6]

Another point which should be mentioned is that

$$\frac{dA}{dx}\approx-C\frac{d^2\phi}{dx^2},\quad C>0 \quad (15)$$

i.e., the first derivative of the amplitude varies in space approximately as the negative second derivative of the phase. This result is a relatively good approximation both in the plane wave and in the narrow-soliton regions.

So far we have considered in the narrow-soliton limit only single-soliton solutions. The discussion can be easily extended to the multisoliton lattice case by assuming that the single-soliton solutions $\phi_s(x)$ and $\Delta A_s(x)$ are additive:

$$\Delta A(x)=\sum_j\Delta A_s(x-jb)\,, \quad (16a)$$

$$\phi(x)=\sum_j\phi_s(x-jb)\,, \quad (16b)$$

where b denotes the intersoliton spacing and $\phi_s(x)$ and $\Delta A_s(x)$ are given by Eqs. (9) and (13).

III. TEMPERATURE DEPENDENCE OF AMPLITUDE VARIATIONS AND SOLITON DENSITY

In order to test the analytical approximations of the preceding section, we calculated the temperature dependence of the amplitude and phase variations—and the soliton density—by solving numerically the Euler-Lagrange equations (2a) and (2b). To simplify the calculation we introduce dimensionless variables for $g(x)$, x, A, and q but retain these notations for convenience. The free-energy density $g(x)$ expressed in new variables now reads

$$g(x)=\frac{\tau}{2}A^2+\tfrac{1}{4}A^4+\frac{\gamma}{\kappa}A^n\cos^2(n\phi)-A^2\phi'+\tfrac{1}{2}(A^2\phi'^2+A'^2)\,, \quad (17)$$

where $\tau=(T-T_0)/(T_I-T_0)$. In this notation we have $q(T_I)=q_0=1$ and $A(T_0)=1$ for $\gamma=0$.

To solve the corresponding Euler-Lagrange equations we used the following ansatz in terms of plane-wave harmonics[3]:

$$\phi'=q+C_1\cos(nqx)+C_2\cos(2nqx)+C_3\cos(3nqx)\,, \quad (18a)$$

$$A=A_0-A_1\cos(nqx)-A_2\cos(2nqx)\,. \quad (18b)$$

Simultaneously, the free energy $F=(1/L)\int_0^L g(x)dx$ was minimized with respect to q to obtain the equilibrium value of q. It should be noted that the wave vector q obtained in this way is not the wave vector which is usually given in the literature—e.g., for Rb_2ZnCl_4, $q_s=(1-\delta)a^*/3$—but $q=\delta/\delta_0$ where δ_0 is the value of δ at T_I. The corresponding wavelength is $\lambda=6\pi/\delta a^*=3a/q\delta_0$. Since $n=6$ for Rb_2ZnCl_4 the intersoliton distance $b=\lambda/n$

$=a/2q\delta_0$.

The calculations were done for $n=6$ with $\gamma/\kappa=0.1$, 0.025, 0.01, and 0.005. They were started near T_I by using the approximations (5), (6), and (8) for C_1, A_0, and A_1 as initial values for the iteration. The calculated values for all coefficients were then extrapolated to obtain the initial values for the next lower temperatures. Simultaneously, the free energy F of the modulated phase was compared with the free energy $F^*=\frac{1}{2}\tau A^2+\frac{1}{4}A^4$ of the lock-in phase. The procedure was stopped at the temperature where F^* became smaller than F. The fact that this happens for all values of γ/κ near $q=0.6$ indicates that the corresponding temperature is in general, not the lock-in temperature, but rather, the temperature where the approximation (18a) and (18b) breaks down.

The results are shown in Figs. 1 and 2. In Fig. 1 the value of the wave vector q and the soliton density n_s are plotted versus temperature for various values of γ/κ. The soliton density n_s is defined as

$$n_s=q/(q+C_1+C_2+C_3)\,, \tag{19}$$

i.e., as the ratio between the average space derivative of the phase $\langle\phi'\rangle$ and $\phi'(x=0)$, i.e., in the middle of a soliton. Here, not only the intersoliton spacing but also the soliton width is taken into account in defining the soliton density. This definition is equivalent to the NMR definition which defines n_s as the ratio between the number of nuclei in the soliton domain walls as compared to the total number of nuclei. The soliton width is thus given by

$$w_s=n_s b=\frac{1}{q+C_1+C_2+C_3}\,\frac{a}{2\delta_0}\,. \tag{20}$$

The dotted curve of $q(T)$ for $\gamma/\kappa=0.1$ is calculated with $A(x)=$const. The temperature where F^* becomes smaller than F is in this case nearly the same as for $A=A(x)$. The state with $A=$const always has a higher free energy than the state with $A=A(x)$. Since the $A=$const curve is thus, for all values of γ/κ, above the curve where amplitude fluctuations are allowed, it is plausible that an extrapolation for a continuous lock-in transition would lead to a too low T_c for $A=$const.

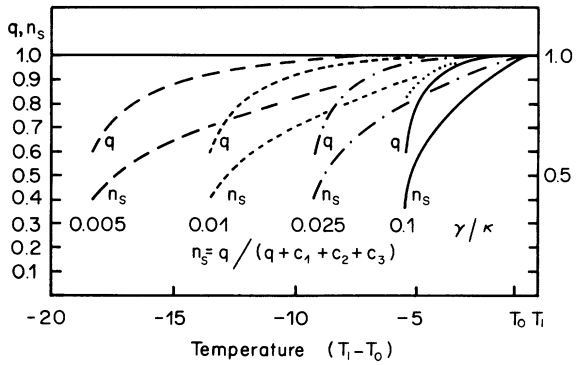

FIG. 1. Temperature dependence of the wave vector q and the soliton density n_s for $\gamma/\kappa=0.005$, 0.01, 0.025, and 0.1 with $A=A(x)$. The dotted curve above the solid line $q(T)$ for $\gamma/\kappa=0.1$ is calculated for $A=$const with the same coefficient γ/κ. The temperature scale on the horizontal axis is expressed in T_I-T_0 units.

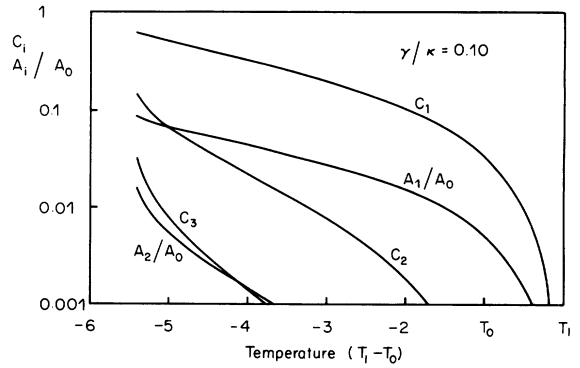

FIG. 2. Temperature dependence of the coefficients C_1, C_2, C_3, A_1/A_0, and A_2/A_0 of Eqs. (18a) and (18b). The temperature scale on the horizontal axis is expressed in T_I-T_0 units.

It should also be mentioned that according to Ref. 4 the lock-in transition is expected to be slightly discontinuous for

$$\frac{T_I-T_c}{T_I-T_0}<25\,.$$

The step in q at T_c should then increase with increasing γ/κ. This was observed in our model calculations only for values of $\gamma/\kappa>0.5$, whereas the discontinuity was too small to be discernible for $\gamma/\kappa<0.5$.

Another important fact to be stressed is that the temperature dependencies of the soliton density n_s and the incommensurate wave vector q are qualitatively different. This is true both for $A=A(x)$ and for the $A=$const approximation. Near T_I, q is nearly constant but drops steeply as T_c is approached. The soliton density n_s, on the other hand, decreases rather smoothly with decreasing temperatures throughout most of the incommensurate phase. Close to T_c it vanishes in the same way as q. The difference is due to the fact that near T_I the soliton width w_s decreases with decreasing temperature faster than the inverse intersoliton spacing $1/b$.

In Fig. 2 the temperature dependence of C_1, C_2, C_3, A_1/A_0, and A_2/A_0 is plotted in a logarithmic scale for $\gamma/\kappa=0.1$. One can see that there is a relation between C_1 and A_1/A_0 which can be obtained

from Eqs. (5) and (8),

$$A_1/A_0 \approx C_1/n \quad (n=6) .$$

It can be seen from Fig. 2 that a similar relation exists between C_2 and A_2/A_0:

$$A_2/A_0 \approx C_2/2n \quad (n=6) .$$

By substituting A_1 and A_2 in our ansatz Eq. (18b), with these relations and taking the first derivative with respect to x for both Eqs. (18a) and (18b), we obtain

$$A'(x) \approx -\phi''(x)/A_0 , \tag{21}$$

which is equivalent to Eq. (15). This relation is illustrated in Fig. 3 where the phase ϕ and the amplitude A are plotted versus x for $\gamma/\kappa=0.43$. The corresponding spatial variation of the two-component order parameter $\tilde{p},\tilde{q}$ is shown below. The atomic displacements $u(x)$ are linear combinations of $\tilde{p}$ and $\tilde{q}$ and can be expressed as

$$u(x) \propto A(x)\cos[\phi(x)+\phi_0] . \tag{22}$$

Here ϕ_0 is a phase shift which can be different for each kind of atom in the system and which cannot be predicted by the continuum Landau theory as it follows from the discrete crystal structure.

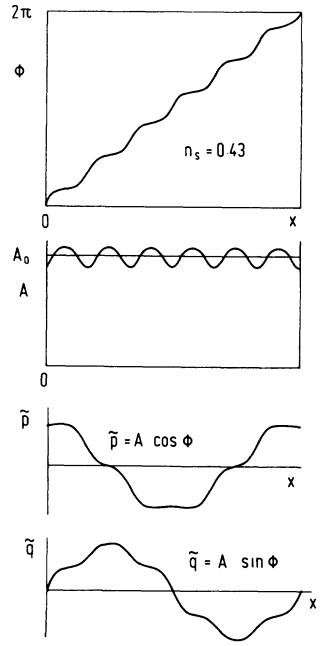

FIG. 3. Spatial variation of the phase ϕ and the amplitude A as well as of the corresponding two-component order parameter $\tilde{p},\tilde{q}$. All atomic displacements $u(x)$ in the crystal are linear combinations of $\tilde{p}$ and $\tilde{q}$.

IV. NMR LINE SHAPE AND AMPLITUDE FLUCTUATIONS

Let us now evaluate the NMR line shape for the case of a pinned modulation wave in the continuum limit.[6] The NMR, nuclear quadrupole resonance (NQR), or EPR frequency reflect[1] the spatial variation of the incommensurate order parameter

$$u = A(x)\cos\varphi(x) , \tag{23a}$$

so that

$$\nu = \nu(u(x)) . \tag{23b}$$

Here $\varphi(x)=\phi_0+\phi(x)$, where ϕ_0 and $\phi(x)$ were introduced in Eqs. (1) and (22).

The inhomogeneous resonance line shape $F(\nu)$ is determined by the convolution of the frequency distribution[1]

$$f(\nu)=\frac{\text{const}}{|d\nu/dx|}=\frac{\text{const}}{|(d\nu/du)(du/dx)|} \tag{24a}$$

with the line-shape function $L(\nu-\nu_c)$ of a single line corresponding to a given site

$$F(\nu)=\int L(\nu-\nu_c)f(\nu_c)d\nu_c . \tag{24b}$$

Using expression (24a) we get the frequency distribution as

$$f(\nu)=\frac{\text{const}}{A\,|-\sin\varphi(d\phi/dx)+\cos\varphi(dA/dx)(1/A)|\,|(d\nu/du)|} . \tag{24c}$$

If the wavelength of the modulation wave is large as compared to the size of the region from where the dominant contribution to the frequency ν comes, $\nu=\nu(u(x))$ can be expanded in powers of the order parameter.

In this case we find

$$\nu=\nu_0+a_1u+\tfrac{1}{2}a_2u^2+\cdots , \tag{25a}$$

and with the help of expression (23a)

$$\nu=\nu_0+a_1A(x)\cos\varphi(x) + \tfrac{1}{2}a_2A^2(x)\cos^2\varphi(x)+\cdots . \tag{25b}$$

The factor $\cos\varphi$ takes on nearly continuously all values between $+1$ and -1 as x runs over all lattice sites which are equivalent in the high-tem-

perature phase.

The singularities in the line shape are determined by the zeros of the derivative

$$\frac{d\nu}{dx}=-\sin\varphi(\nu_1+\nu_2\cos\varphi+\cdots)\frac{d\phi}{dx}+\cos\varphi(\nu_1+\nu_2\cos\varphi+\cdots)\frac{dA}{dx}\frac{1}{A}\,. \quad (26)$$

Here we introduced

$$\nu_1=a_1A_0,\ \nu_2=a_2A_0^2,\ldots\,. \quad (27)$$

The term dA/dx in Eqs. (24c) and (26)—reflecting the space variations of A—has not yet been taken into account in comparing experimental magnetic-resonance data with theoretical models.[1] In the "plane-wave" limit when $d\phi/dx=q_0$, $d^2\phi/dx^2=0$, this term is indeed negligible. In other cases it may, however, significantly affect the resonance line shape.

In the plane-wave-regime case we find for $a_1\neq 0$, $a_2=a_3=0$,

$$f(\nu)=\frac{\text{const}}{|\sin\varphi[1-K_1\cos(n\phi)]+n(A_1/A_0)\cos\varphi\sin(n\phi)|}\,, \quad (28)$$

where $\phi=q_0x$ and $K_1=[\gamma\kappa/(2\Lambda^2)]\,A_0^{n-2}$. For $n=6$, for instance, we thus get for $\phi_0=0$,

$$f(\nu)=\text{const}\left[\left[1-\left[\frac{\nu-\nu_0}{\nu_1}\right]^2\right]^{1/2}\left[1+6\left[\frac{\nu-\nu_0}{\nu_1}\right]\left\{32\frac{A_1}{A_0}\left[\left[\frac{\nu-\nu_0}{\nu_1}\right]^4-\left[\frac{\nu-\nu_0}{\nu_1}\right]^2+\frac{6}{32}\right]\right\}-K_1\left[32\left[\frac{\nu-\nu_0}{\nu_1}\right]^6-48\left[\frac{\nu-\nu_0}{\nu_1}\right]^4+18\left[\frac{\nu-\nu_0}{\nu_1}\right]-1\right]\right]\right]^{-1}. \quad (29)$$

The frequency distribution still has the characteristic square-root-type edge singularities[1] at $\nu=\nu_0\pm\nu_1$, as obtained in the plane-wave limit for $A=$const, but the shape of the distribution is changed. The magnitude of the change depends on A_1 and K_1 and is small in this case.

In the multisoliton lattice case[1,7] we find in the $A=A_0$ approximation $d\phi/dx$ from the sine-Gordon equation as

$$\frac{d\varphi}{dx}=\text{const}\left[\Delta^2+\cos^2\frac{n(\varphi-\phi_0)}{2}\right]^{1/2}, \quad (30)$$

where ϕ_0 stands for the initial phase of the modulation wave and Δ is related to the soliton density (i.e., the fraction of nuclei in the incommensurate domain walls) as

$$n_s=\frac{\pi/2}{K[1/(1+\Delta^2)^{1/2}]}\,. \quad (31)$$

Here K is the complete elliptic integral of the first kind. Expression (31) is in fact identical with Eq. (18). The value of n_s is 1 in the plane-wave limit where $\Delta\gg 1$ and approaches zero when $\Delta\ll 1$. Expression (30) yields, together with expression (24c) for $A=$const, up to n new commensurate lines for $\Delta\to 0$ in addition to the incommensurate edge singularities. The new lines appear[8-10] for $\Delta\ll 1$ when $\cos^2 n(\varphi-\phi_0)/2=0$, i.e., when

$$\varphi=(2m+1)\pi/n+\phi_0,\quad m=0,1,2,\ldots,n-1 \quad (32)$$

whereas the edge singularities will appear when $\sin\varphi=0$, so that φ is an integer multiple of π.

Close to T_c, where the solitons are far apart, we can evaluate the amplitude variation over an isolated phase soliton centered at $x=0$ from expression (14) as

$$\frac{1}{A_0}\frac{dA}{dx}\approx-\frac{1}{\xi}\frac{dG}{dx}\,, \quad (33)$$

yielding

$$\frac{1}{A_0}\frac{dA_s}{dx}=\frac{\pi\Lambda^2A_0l}{\xi\kappa}\times\left[\frac{(n+2)\pi}{4}\frac{1}{\cosh(lx)}-1\right]\frac{\tanh(lx)}{\cosh(lx)}\,, \quad (34)$$

where

$$l=n(\gamma A_0^{n-2}/2\kappa)^{1/2}=w_s^{-1} \quad (35)$$

is the inverse soliton width.

For a multisoliton lattice we get in this approximation, where the intersoliton spacing b is large as compared to the soliton width w_s,

$$\frac{1}{A_0}\frac{dA}{dx}=\sum_j\frac{1}{A_0}\frac{dA_s}{dx}(x-jb)\,, \quad (36)$$

with dA_s/dx standing for the derivative of the single-soliton solution as given by Eq. (34). In the same approximation we have from (9a)

$$\phi'(x)=\sum_j \phi_s'(x-jb)\ , \tag{37}$$

with

$$\phi_s'=\frac{2l}{n\cosh(lx)} \tag{38}$$

being the derivative of the single-soliton solution (9a). Putting expressions (37), (38), (36), and (34) into expression (24c) we get the frequency distribution function in the "narrow" soliton limit as $T\rightarrow T_c$.

The results of a numerical evaluation of the magnetic-resonance line shape $F(\nu)$ in the presence of amplitude variations $A=A(x)$ are presented in Fig. 4 for $n=6$ and $\phi_0=0,90°$, and for soliton densities $n_s=1$, 0.9, 0.8, 0.7, 0.6, 0.5, and 0.4. Here we assumed that $a_1\neq 0$, $a_2=a_3=0$. The line shapes $f(\nu)$ have been convoluted with a Lorentzian the width of which was 2.5% of $2\nu_1$. The gradual appearance of the commensurate lines for $n_s<0.9$—occurring in addition to the "incommensurate" edge singularities at $\nu=\pm\nu_1$— is clearly seen. For a general ϕ_0 we have six commensurate lines and two incommensurate edge singularities. At least two of the commensurate lines occur so close to the two edge singularities that they cannot be separated from them in view of the finite Lorentzian linewidth (Fig. 5). The intensities at $\nu=\pm\nu_1$ should be thus continuous at T_c. For special values of ϕ_0 (i.e., $\phi_0=30°,0°$ in the case $n=6$), some of the commensurate lines merge so that, e.g., for the $\phi_0=0$, two of the commensurate lines occur at the center, and four coincide with the edge singularities.

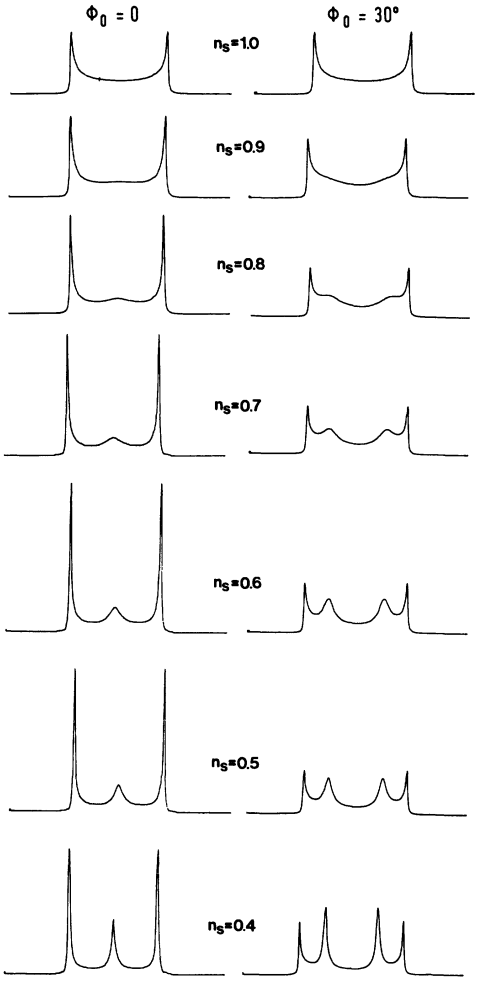

FIG. 4. Magnetic-resonance line shape for a linear dependence of ν_Q on $u(x)$ for various soliton densities n_s. The curves for $\phi_0=0$ correspond to the frequency density $f(\nu)$ obtained from $\tilde{p}(x)$, the ones with $\phi_0=30°$ to $f(\nu)$ obtained from $\tilde{q}(x)$. The spectral densities $f(\nu)$ are convoluted with a Lorentzian of the width $0.05\nu_1$.

In Fig. 6 the theoretical magnetic-resonance line shapes for $A=A(x)$ and $A=\text{const}$ are compared for $n_s=0.6$, $\phi_0=0,30°$, and $n=6$. Amplitude variations clearly affect the relative positions of both the edge singularities and the commensurate lines. For $\phi_0=0$, amplitude variations produce a merging of the edge singularities and commensurate lines so that we have three peaks in $F(\nu)$ instead of the five

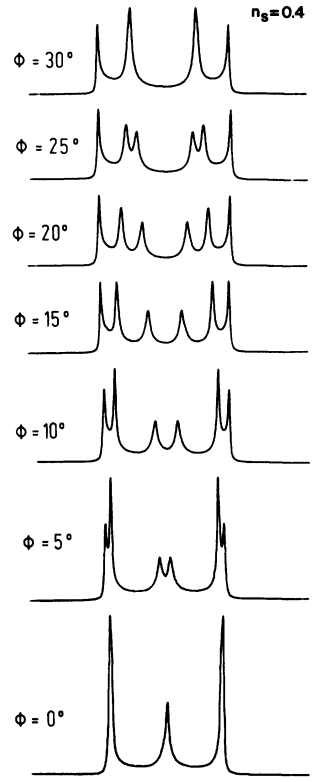

FIG. 5. Magnetic-resonance spectra for various initial phases ϕ_0 for the case $n_s=0.4$ in Fig. 4.

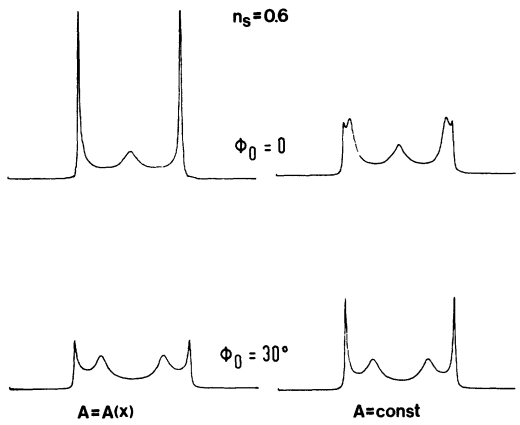

FIG. 6. Comparison between the NQR spectra for $A=A(x)$ and $A=$const in the case of a soliton density $n_s=0.6$ for $\phi_0=0$, 30°.

expected in the $A=$const approximation. In addition, the commensurate lines are significantly narrowed as expected from the $\tilde{p}=\tilde{p}(x)$ curve in Fig. 3. The effect is just the opposite for $\phi_0=30°$. Here both the edge singularities and commensurate lines broaden under the influence of amplitude variations. This effect can again be seen from the $\tilde{q}=\tilde{q}(x)$ curve in Fig. 3.

One may thus conclude that amplitude variations—occurring in addition to phase solitons—significantly affect the NMR line shape for soliton densities n_s which are smaller than 0.7. These effects are absent close to T_I where we are in the "plane-wave" regime. Amplitude variations are particularly important in the "narrow" soliton range close to T_c. For $\phi_0=0$, for instance, with decreasing soliton density the "incommensurate" singularities move away from the edges toward the center and simultaneously become weaker. At the edges of the spectrum we can have now commensurate lines. The intensity of the incommensurate background is as well reduced. The effects, of course, again depend on ϕ_0. Amplitude variations must be thus taken into account when one tries to determine quantitatively the temperature variation of the solition density very close to T_c. Though a detailed comparison of the above theory with experimental data is reserved for a planned subsequent paper it should be nevertheless mentioned that the temperature dependence of the incommensurate wave vector in Rb_2ZnCl_4 and the observed Rb magnetic-resonance line shapes in Rb_2ZnBr_4 closely resemble those predicted by the above model for $n=6$.

[1]For a review of NMR in I systems see R. Blinc, Phys. Rep. 79, 331 (1981), and references therein.

[2]R. A. Cowley, Adv. Phys. 29, 1 (1980), and references therein.

[3]H. Shiba and Y. Ishibashi, J. Phys. Soc. Jpn. 44, 1592 (1978).

[4]A. E. Jacobs and M. B. Walker, Phys. Rev. B 21, 4132 (1980); P. Prelovšek, J. Phys. C 15, L269 (1982).

[5]Y. Ishibashi, Ferroelectrics 24, 119 (1980).

[6]D. A. Bruce, J. Phys. C 13, 4615 (1980).

[7]A. S. Chaves, R. Blinc, J. Seliger, and S. Žumer, J. Magn. Reson. 46, 146 (1982).

[8]R. Blinc, V. Rutar, B. Topič, F. Milia, I. P. Aleksandrova, A. S. Chaves, and R. Gazzinelli, Phys. Rev. Lett. 46, 1406 (1981).

[9]B. H. Suits, S. Couturie, and C. P. Slichter, Phys. Rev. Lett. 45, 194 (1980).

[10]R. Blinc, I. P. Aleksandrova, A. S. Chaves, F. Milia, V. Rutar, J. Seliger, B. Topič, and S. Žumer, J. Phys. C 15, 547 (1982).